

A Comparative Study of Mouse Liver Proteins Arylated by Reactive Metabolites of Acetaminophen and Its Nonhepatotoxic Regioisomer, 3'-Hydroxyacetanilide

Timothy G. Myers,[†] Eric C. Dietz,[‡] N. Leigh Anderson,[§] Edward A. Khairallah,^{||} Steven D. Cohen,[⊥] and Sidney D. Nelson^{*,‡}

Department of Medicinal Chemistry, BG-20, University of Washington, Seattle, Washington 98195, Large Scale Biology Corporation, Rockville, Maryland 20850, Department of Molecular and Cell Biology, University of Connecticut, Storrs, Connecticut 06268, and Department of Pharmacology and Toxicology, University of Connecticut, Storrs, Connecticut 06268

Received May 20, 1994[®]

Acetaminophen (4'-hydroxyacetanilide), a widely used analgesic/antipyretic drug, is hepatotoxic in large doses, whereas the *m*-hydroxy isomer of acetaminophen, 3'-hydroxyacetanilide, is not hepatotoxic. Both are oxidized by mouse liver cytochromes P-450 to reactive metabolites that bind covalently to hepatic proteins. Because previous studies have shown that peak levels of liver protein adducts formed after the administration of each of these compounds to mice are nearly equivalent, and because liver protein adduct formation correlates with hepatotoxicity caused by acetaminophen in mice, we investigated the abundance and patterns of protein adducts formed by acetaminophen and its regioisomer for significant differences. Hepatotoxic doses of acetaminophen to mice significantly altered the abundances of several liver proteins 2 h after dosing as revealed by densitometric analysis of two-dimensional electrophoretic patterns of these proteins. The same analysis after the administration to mice of 3'-hydroxyacetanilide indicated that this nonhepatotoxic regioisomer of acetaminophen caused several similar changes in protein patterns, but also revealed some significant differences. Binding of radiolabeled acetaminophen and 3'-hydroxyacetanilide to hepatic proteins corroborated and extended these results. Two hours after the administration of ¹⁴C-labeled analogs of these two compounds to mice, at a time when their extent of total covalent binding to hepatic proteins is approximately equivalent, there are many similarities but also some differences in selectivity of proteins that are adducted, as revealed by both one-dimensional and two-dimensional gel electrophoresis followed by phosphorimage analysis of radiolabel bound to protein bands. Moreover, protein adducts formed from 3'-hydroxyacetanilide were found to be less stable than those formed from acetaminophen under the conditions of electrophoretic analysis. Furthermore, a comparison of radiodetection and immunodetection of protein adducts formed from acetaminophen with an antibody specific for acetaminophen protein adducts indicates that the antibody detects most of the same proteins that are radiolabeled and that the relative quantitative contribution of various adducts to the overall covalent binding of acetaminophen to proteins is approximately the same by both methods. Thus, 3'-hydroxyacetanilide should prove to be a useful tool to aid in the discrimination of hepatic acetaminophen protein adducts that may be critical or noncritical to survival of hepatocytes.

Introduction

Acetaminophen (4'-hydroxyacetanilide, paracetamol, APAP)¹ is a widely used analgesic/antipyretic that after large doses can cause severe centrilobular liver necrosis in animals and humans (1–5). There is substantial evidence that the hepatotoxicity is mediated primarily

by the cytochrome P-450 oxidative metabolite, *N*-acetyl-*p*-benzoquinone imine (NAPQI) (6–12). NAPQI both arylates and oxidizes cysteinyl thiol groups in small peptides and proteins (7, 13), and both mechanisms, as well as others, may be involved in the pathogenesis of hepatotoxicity caused by APAP (for recent reviews see refs 14–16).

One long-standing hypothesis has been that the covalent binding of oxidative metabolites of APAP to proteins in the liver modifies their normal function and initiates processes that culminate in cell death (17, 18). Based on mass spectrometric analysis of hepatic proteins from mice, the cysteinyl thiol group is the major site of protein adduction by APAP metabolites (19). However, 3'-hydroxyacetanilide (AMAP) is a nonhepatotoxic regioisomer of APAP whose oxidative quinone and quinone imine metabolites bind to cysteinyl thiol groups of mouse liver to approximately the same extent as reactive metabolites of APAP (20). Therefore, if covalent binding plays a role in the pathogenesis of liver damage, there

* To whom correspondence should be addressed.

[†] Present address: Laboratory of Molecular Pharmacology, Developmental Therapeutics Program, National Cancer Institute, Bethesda, MD 20892.

[‡] University of Washington.

[§] Large Scale Biology Corp.

^{||} Department of Molecular and Cell Biology, University of Connecticut, Storrs, CT 06268.

[⊥] Department of Pharmacology and Toxicology, University of Connecticut, Storrs, CT 06268.

[®] Abstract published in *Advance ACS Abstracts*, March 1, 1995.

¹ Abbreviations: APAP, acetaminophen or 4'-hydroxyacetanilide; AMAP, 3'-hydroxyacetanilide; NAPQI, *N*-acetyl-*p*-benzoquinone imine; LSC, liquid scintillation counting; LSB, Large Scale Biology Corp.; SDS-PAGE, sodium dodecyl sulfate-polyacrylamide gel electrophoresis; DTT, dithiothreitol; PMSF, phenylmethanesulfonyl fluoride; IEF, isoelectric focusing.

must be some difference in the covalent binding of APAP and AMAP to hepatic proteins. In fact, on a subcellular level, reactive metabolites of APAP have been found to bind more extensively to mouse liver proteins in the mitochondrial and nuclear compartments than reactive metabolites of AMAP, whereas the reverse is the case for proteins in the cytosolic and microsomal compartments (21). Thus, an important objective is to identify and characterize specific protein adducts.

One method that has been successfully used to demonstrate that APAP binds to selective proteins in mouse liver after hepatotoxic doses is immunochemical detection with affinity-purified antibodies (22–28). Several proteins in each subcellular fraction of mouse liver and some human livers have been found to form immunodetectable adducts with acetaminophen. A few hepatic proteins that have recently been found to form adducts with APAP reactive metabolites after the administration of hepatotoxic doses of APAP to mice include a cytosolic selenium binding protein (29, 30), a microsomal subunit of glutamine synthetase (31), the cytosolic protein *N*-10-formyltetrahydrofolate dehydrogenase (32), and the nuclear protein lamin A (33).

Though the use of immunodetection techniques provides a very useful approach to characterize protein adducts of APAP, there are some potential drawbacks. First, the antibodies used may not access and/or recognize some adducts. Second, immunodetection may not accurately reflect the amount of any given adduct because the extent of adduct recognition may vary from protein to protein. Finally, and irrespective of the methodology used, the detection and identification of a particular protein adduct do not necessarily implicate a role for the modification in a pathogenic process.

In this report, we describe results of studies that utilized both one- and two-dimensional (1- and 2-D) gel electrophoresis and radiodetection of adducts for a more complete assessment of the spectrum of proteins arylated by APAP reactive metabolites. Furthermore, comparisons are made between proteins that are arylated by reactive metabolites of APAP and AMAP to provide an approach to aid in the selection of proteins that may be critical targets in the pathogenesis of hepatotoxicity caused by APAP.

Experimental Procedures

Materials. APAP and AMAP were purchased from Aldrich Chemical Co. (Milwaukee, WI) and recrystallized before use (ethanol/water, 1:1). Sigma Radiochemicals (St. Louis, MO) supplied [*ring*-U-¹⁴C]APAP (10.2 mCi/mmol) and [*ring*-U-¹⁴C]-AMAP (16.2 mCi/mmol). The radiochemical purity of both compounds was greater than 97%, as determined by HPLC on a reverse phase 5 μ m Ultrasphere ODS column (25 cm \times 10 mm; Rainin Instruments, Berkeley, CA) protected by a 5 μ m Ultrasphere precolumn. Elution was isocratic with water/acetonitrile/glacial acetic acid (800:180:20 v/v) at a flow rate of 2 mL min⁻¹.

[*acetyl*-1-¹⁴C]APAP (1.76 mCi/mmol) was prepared from [1-¹⁴C]acetic acid (Sigma Radiochemicals) and *p*-aminophenol. [1-¹⁴C]Acetylimidazole was prepared by reacting a solution of [1-¹⁴C]acetic acid (5 mg, 0.08 mmol, 10 mCi/mmol) in 400 μ L of dry ether with *N,N'*-carbonyldiimidazole (10 mg, 0.12 mmol). After complete dissolution of *N,N'*-carbonyldiimidazole and effervescence had ceased, 1 mL of absolute ethanol was added followed by *p*-aminophenol (13 mg, 0.09 mmol) and stirring for 30 min. Excess carbonyldiimidazole was destroyed by addition of 1 mL of 1 M HCl. The mixture was extracted with ethyl acetate, and ethyl acetate extracts were dried over Na₂SO₄. The drying agent was removed by filtration, and remaining solvent was removed *in vacuo*. The product [*acetyl*-1-¹⁴C]APAP was

purified by HPLC as described above. The overall yield of purified product was 30% with sp act. of 7.3 mCi/mmol. **Caution:** Care should be taken in the handling of phenol which is toxic and corrosive, *p*-aminophenol which is toxic and an irritant, and *N,N'*-carbonyldiimidazole which is corrosive.

Animals. Both B6C3F1 and Swiss-Webster male mice 6 weeks of age (20–30 g) were obtained from Charles River Laboratories (Wilmington, MA) and maintained on Purina 5001 rodent chow. Food was withheld from all mice 12–16 h prior to the administration of drugs. B6C3F1 mice were used for the 2-D comparative studies carried out by Large Scale Biology Corp. (LSB; Rockville, MD) using their proprietary ISO-DALT System that incorporates a master pattern of proteins for this inbred mouse strain which has less allelic variants than the outbred Swiss-Webster strain. Both APAP and AMAP were given *ip* as saturated aqueous solutions at doses of 600 mg/kg to the B6C3F1 mice. Results of pilot studies showed that this dose of APAP was hepatotoxic whereas the same dose of AMAP was not, though both bound equivalently to hepatic proteins 2 h after dosing. In studies with radiolabeled drugs, male Swiss-Webster mice were given phenobarbital as a 0.1% solution in their drinking water for 5 days prior to treatment. In this way lower doses of APAP could be administered to save on radiolabel. A toxic dose of APAP was determined to be 250 mg/kg, the highest dose tolerated without observable mortality. The highest tolerated dose of AMAP was 600 mg/kg. Higher doses of AMAP caused fatal respiratory depression, but not hepatotoxicity.

Subcellular Fractionation. Two hours after dosing, the animals were killed by cervical dislocation. Livers were excised surgically, weighed, and homogenized with a Potter-Elvehjem type homogenizer. A portion of the homogenate was retained, and the remainder was subjected to differential centrifugation according to a previously reported scheme (21). Supernatant fractions were immediately frozen to -70°C . Pelleted fractions were resuspended in a small amount of buffer (final protein concentrations 20–30 mg/mL) before freezing to -70°C . All samples were stored at -70°C until further use.

Covalent Binding. Gross covalent binding was determined as previously described (20). Protein concentrations were determined using the Micro-BCA assay from Pierce (Rockford, IL) and bovine serum albumin as standard.

SDS-PAGE Electrophoresis. Sodium dodecyl sulfate-polyacrylamide gel electrophoresis (SDS-PAGE) was conducted according to the method of Laemmli (34). The stacking gel was 3% acrylamide, and the running gel was 10% acrylamide. All gels were run under reducing conditions with dithiothreitol (DTT) added to the sample buffer. The gel dimensions were 0.15 \times 12 \times 15 cm long (Hoefer SE600) and were run at 20 mA per gel, constant current, at room temperature. Typically, 10 samples (100–600 μ g/lane) were loaded per gel.

Protein fractions were solubilized in 62 mM Tris buffer (pH 6.8), containing 1% SDS, 10 mg/mL DTT, and 10% glycerol. Before loading, the samples (in microfuge tubes) were heated in boiling water for 2–5 min and centrifuged, 14 000 rpm for 5 min, to remove any insoluble matter.

Protein Staining. Protein bands were made visible by staining the gels with Coomassie Blue R-250 (0.5% w/v) in 30% methanol/10% acetic acid/water (v/v) overnight with shaking. Destaining involved several changes of 30% methanol/10% acetic acid/water (v/v).

Electrotransfer. When proteins were transferred to nitrocellulose (Schleicher and Schuell, Inc., Keene, NH), the SDS-PAGE gels were immediately equilibrated in transfer buffer (35) (0.250 M Trizma base, 0.192 M glycine). Transfer was performed in chilled buffer using 1.2 A constant current (Hoefer TE42) for 4 h. Typically, the membrane was saturated to the extent that protein appeared on the distal side of the membrane.

These overloaded gels were run at room temperature and did not give perfectly linear plots of log (MW) vs R_f for MW standards obtained from Sigma (myosin, 205 kDa; β -galactosidase, 116 kDa; phosphorylase-*b*, 97.4 kDa; bovine serum albumin, 66 kDa; egg albumin, 45 kDa; carbonic anhydrase, 29 kDa; trypsinogen-phenylmethanesulfonyl fluoride (PMSF), 24 kDa; soybean trypsin inhibitor, 20.1 kDa; β -lactoglobulin, 18.4

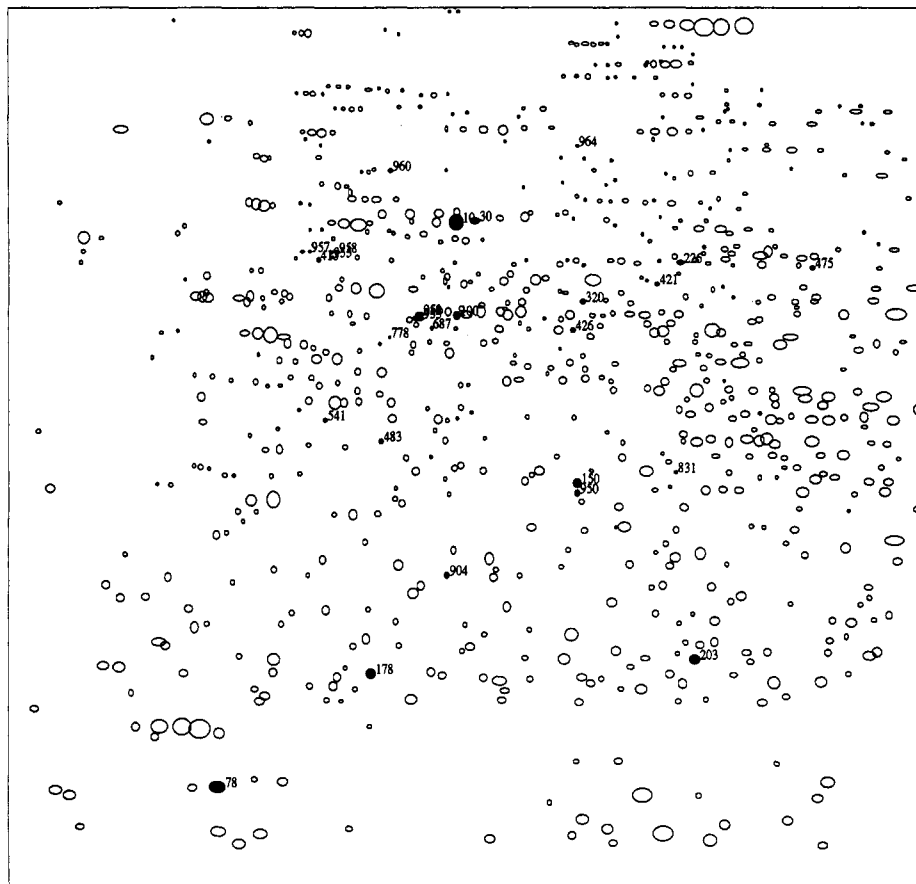


Figure 1. A schematic figure showing the locations of spots significantly changed by AMAP or APAP in B6C3F1 mouse liver. Each liver protein is plotted as an ellipse. Proteins showing significant change ($p < 0.001$ or presence/absence difference) are shown as filled ellipses with associated spot numbers. Major spot 10 is serum albumin, spot 78 is cytochrome b5, and the row of large spots at the upper right is carbamyl phosphate synthase. Two groups of labeled spots have members so close as to partially overlap (a group consisting of spots 957, 413, 955, and 958 in the upper left quadrant, and a group consisting of spots 778, 952, 953, 687, and 100 nearer the center of the pattern). The pattern shows proteins ranging in mass from about 14 (bottom) to 180 kDa (top), and isoelectric point about 4.5 (left) to 7 (right).

kDa; α -lactalbumin, 14.2 kDa). Therefore, the following strategy was adopted for estimating the dalton size (molecular mass) of the bands and spots of interest. Three standard curves were used: one for bands of R_f of 0.2 or less; one for bands of R_f 0.2–0.8; and one for those of 0.8 or greater. We have the greatest confidence in the protein size estimates for bands where the R_f is between 0.2 and 0.8 (20–80% migration).

Electroelution from SDS–PAGE Gels. SDS–PAGE was conducted using 5 mm diameter tube gels and carried out essentially the same as with the slab gels. Power was applied at a constant current of 2.5 mA/gel tube. Gels were isolated by extrusion and cut into 1 cm long sections. Sections were placed in individual Centricon-10 units (Amicon, 10 000 MW cutoff) and eluted for 4 h using SDS–PAGE tank buffer. Eluted proteins were repetitively washed and isolated by ultrafiltration using the same Centricon-10 units and 50 mM potassium phosphate buffer (pH 7.4), until the radioactivity in the filtrate was the same as background.

Two-Dimensional Gel Electrophoresis. Two-dimensional [isoelectric focusing (IEF) SDS–PAGE] electrophoresis was performed essentially as described by O'Farrell (36).

Sample Preparation. The sample preparation protocol described by Anderson et al. (37) was used. Approximately 200 mg of tissue from the left lobe of the liver was homogenized in 1.6 mL of a solubilizing solution of 9 M urea, 2% Nonidet P-40 detergent, 0.5% dithiothreitol, and 2% pH 9–11 ampholytes (LKB). The solubilized protein was centrifuged at 100000g for 30 min, and the supernatant was removed and stored frozen in 1.5 mL microfuge tubes for shipment to LSB. Detailed methods used by LSB for 2-D gel electrophoresis, staining, and computer analysis of the gels have been reported previously (37–40).

Sample preparation for 2-D electrophoresis of radiolabeled proteins was essentially the same with slight modifications. To 1 mL of protein fraction (10–25 mg of protein/mL of buffer) were added 25 μ L of 10% Emulgen 911, 250 μ L of 10% Nonidet P-40, 40 mg of DTT and 1.3 g of urea. The sample was vortexed after each addition. The sample was then allowed to sit at room temperature for 2–4 h for complete solubilization before centrifugation at 16000g for 5 min prior to loading to remove insoluble matter.

Isoelectric Focusing Gels. The IEF gels (5 mm diameter) were 9 M urea, 4% acrylamide, 2% Nonidet P-40, and 1% ampholytes (Bio-Rad 3–10:Bio-Rad 5–7, 1:1). Final volume of each gel was 2.5 mL. The cathode buffer was 10 mM NaOH, and the anode buffer was 10 mM phosphoric acid. After prefocusing the gels for 1 h (200 V for 15 min, 400 V for 15 min, and 800 V for 30 min), the samples (40 μ L, 1 mg of protein) were underlaid at the (unrinsed) cathode surface. An 800 V potential was maintained overnight and increased to 1000 V for 1 h before extruding the gels. The volt-hour total was 12–13 kV h for the 12 cm long gels. Tube gels that were not used immediately were extruded and then frozen in capped tubes to -20°C .

Sizing Gel. The SDS–PAGE gel used for the separation by molecular weight was 10% acrylamide, as above, poured to the top of the glass cassette. A 1% agarose solution (1% agarose, 0.1% SDS, 0.125 M Tris, pH 6.8) at 70 $^\circ\text{C}$ was used to join the IEF tube gel to the top of the SDS–PAGE gel. Before use, the IEF gel containing the focused sample was equilibrated in 50–100 gel volumes of SDS–PAGE sample buffer (2% SDS, 62 mM Tris, pH 6.8, 30 mM DTT) for 1 h at room temperature. SDS–PAGE was run at 20 mA per gel, constant current.

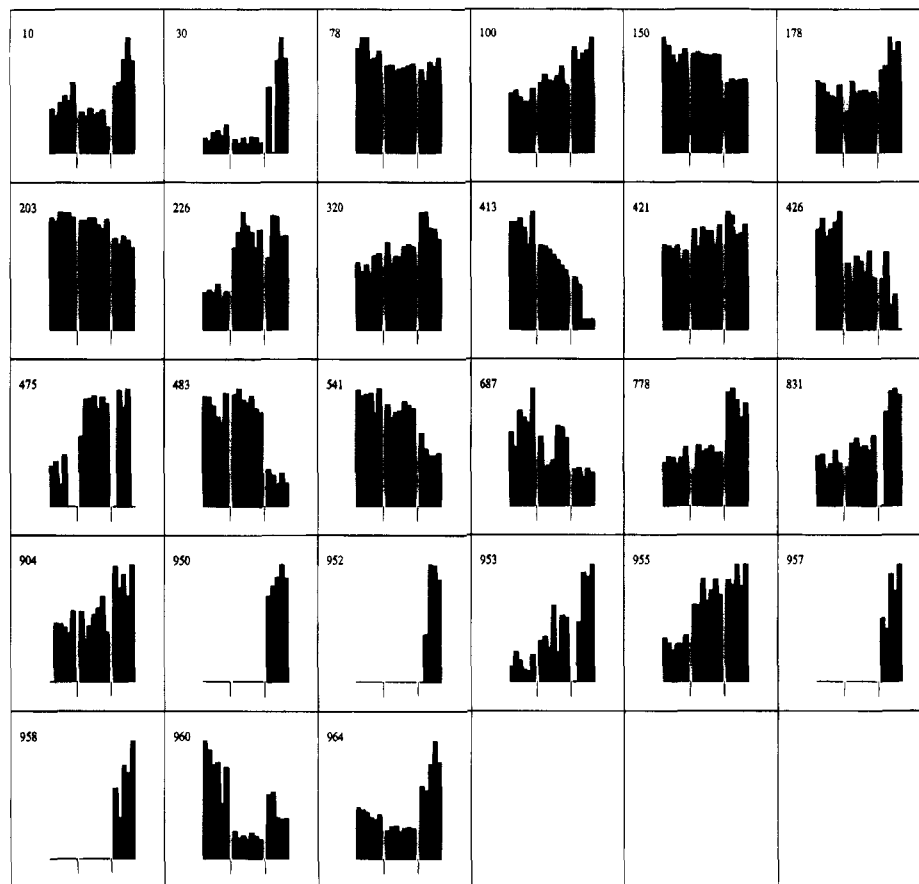


Figure 2. A series of bar-graph panels, one for each of the 27 mouse liver proteins indicated in Figure 1 that showed significant changes in intensity ($p < 0.001$). Each bar represents the abundance on one gel of the protein whose number is shown in the panel's upper left corner. The bars are grouped into three sets, corresponding to the groups in the experiment (controls, AMAP, and APAP treated, respectively, from left to right). Complete statistical analysis of these results is available in table form from the corresponding author as are original panels of the 2-D gel images. For each protein, the results are normalized so that the maximum observed abundance results in a bar of the same height.

Quantitative Analysis of ISO-DALT Gels (LSB). The Kepler software system was used to analyze digitized images of three groups of 2-D gels: group 1 consists of duplicate gels of each of 3 samples from 3 control animals (total 6 gels), group 2 consists of 1 sample from one animal and triplicate gels of each of 2 other AMAP treated animals (total 7 gels), and group 3 consists of duplicate gels of one and triplicate gels of another APAP treated animal (total 5 gels of 2 animals). In the three groups thus defined, there were (after matching to the B6C3F1 mouse liver 2-D master pattern B6C3F1MST2) 231, 282, and 244 spots, respectively, with CV (SD/mean) less than 15%. The gels were scaled together (to eliminate loading differences) using a linear approach prior to statistical analysis using the Student t -test.

Autoradiography Using the PhosphorImager. Autoradiograms were obtained with a Molecular Dynamics PhosphorImager. Nitrocellulose blots and dried gels were exposed for 2–4 days after which the phosphor storage screen was scanned at 88 μm resolution. SDS-PAGE (1-D) lane images were intensity-averaged over the width of the lane using Molecular Dynamics software. The intensity values along the remaining dimension were transferred to a Microsoft Excel spreadsheet. A value for the background intensity was subtracted from the spreadsheet cells before printing the graph in bar-chart format.

Results

Comparisons of Proteins in the ISO-DALT System. Quantitative analysis of Coomassie Blue stained 2-D gels of liver proteins obtained 2 h after treatment of B6C3F1 mice with a hepatotoxic dose of APAP or with AMAP revealed 27 protein spots that differed significantly (t -test $p < 0.001$) from controls (Figure 1). Inter-

estingly, most of the significant changes caused by AMAP occurred in a subset of proteins modified by APAP (Figure 2). A detailed comparison of the two compounds' effects indicates that 6 of the 9 proteins affected by AMAP are also affected by APAP at $p < 0.001$ and that the remaining 3 proteins also show changes in APAP at lower levels of significance (0.008–0.0011). Eight of the 9 proteins change in the same direction (increase or decrease) with both compounds. APAP caused quantitative alterations in 20 protein spots and, in addition, caused the appearance of 4 spots not seen either in controls or in AMAP treated animals (spots numbered 950, 952, 957, 958). The combined total for the two compounds is thus 27 spots, of which more than one-fourth (778, 687, 952, 953, 100, 426, 320) occur in a molecular weight band between the $F_1\text{ATPase } \beta$ subunit (MW = 52K) and HSP60 (MW = 58K).

Only a few of these protein spots have been identified: 78 is cytochrome *b5* (which is decreased approximately 20% by both compounds) while 10 and 30 are isoforms of circulating serum albumin. The changes in albumin probably represent differences in blood content of the liver, consistent with increases (at lower than $p < 0.001$ significance) in spots tentatively identified as apo A-1 lipoprotein and α -1-antitrypsin (other major plasma proteins). The intensities of other identified proteins (e.g., actin, tubulin, protein disulfide isomerase, HSP 90, ornithine decarboxylase, and epoxide hydrolase) did not significantly change.

Table 1. Covalent Binding to Mouse Liver Homogenate Protein Two Hours Post-Injection

label-compd	dose (mg/kg)	sp act. (mCi/mmol)	covalent binding (nmol/mg)
ring-AMAP	600	3.21	1.25
ring-APAP	250	3.57	1.82
acetyl-APAP	250	1.76	1.79
ring-APAP	125	8.39	0.25

Covalent Binding to Mouse Liver Homogenate Proteins. The 2 h time point was chosen based on the results of earlier experiments (20, 21). Phenobarbital-induced mice administered 250 mg/kg doses of APAP develop extensive centrilobular necrosis by 24 h that is preceded by binding of radiolabel that peaked between 1 and 3 h post-injection. Phenobarbital-induced mice administered AMAP (600 mg/kg) had comparable levels of covalent binding, but hepatotoxicity did not develop. Covalent binding of radiolabel from AMAP peaked between 1 and 2 h. Therefore, we chose to isolate livers from mice 2 h post-injection, a time when both compounds would have nearly peak binding.

Ring-labeled and acetyl-labeled APAP were administered to different mice in toxic doses to determine the extent to which electrophoretically isolable protein adducts retained the *N*-acetyl group. A third treatment consisted of a nontoxic dose of APAP (125 mg/kg). Submaximal doses of APAP have been shown to cause detectable covalent binding without complete depletion of glutathione (18).

Covalent binding levels to liver homogenate proteins of ring-labeled APAP and AMAP (Table 1) were comparable to those observed in our earlier experiments with mice (20, 21). The acetyl group apparently was retained in most of the protein adducts, though it must be borne in mind that the data were obtained from individual mice. Binding after the lower dose of APAP was only 15% of that following a toxic dose. On the basis of previous studies (17), hepatic necrosis is not observed in mice after receiving doses of acetaminophen that generate these low levels of protein adducts.

SDS-PAGE of Proteins from Liver Cytosol. Liver cytosol was subjected to SDS-PAGE, and then the

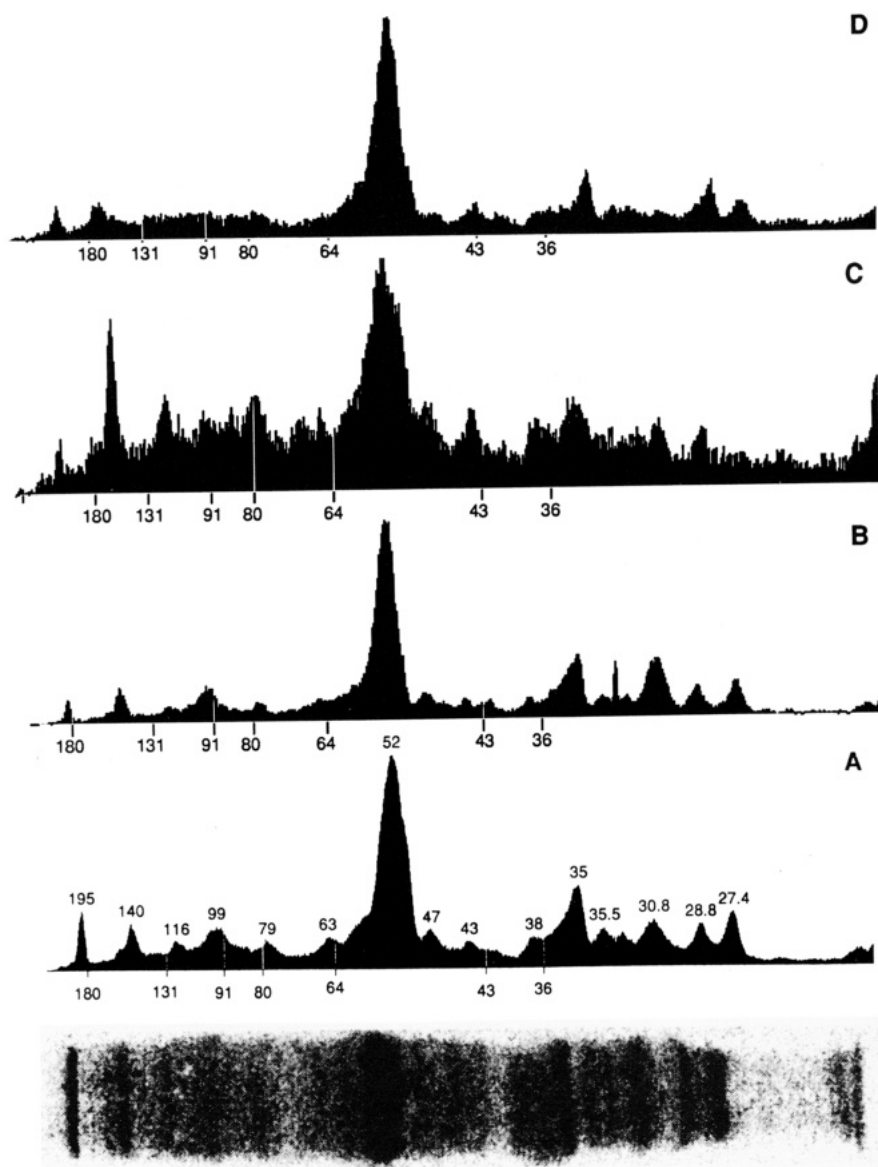


Figure 3. Protein adducts in mouse liver cytosol. Radioactivity profiles obtained by storage phosphorimage analysis of proteins separated by denaturing SDS-PAGE and transferred to nitrocellulose. Samples contained $\sim 700 \mu\text{g}$ of protein from mice treated with the compounds in Table 1. (A) Ring-APAP; (B) acetyl-APAP; (C) AMAP; (D) low-dose APAP. Hash marks below the profiles indicate the positions of molecular mass standards, 180, 131, 91, 80, 64, 43, and 36 kDa, that were run in a parallel lane. Peaks are annotated with the corresponding molecular mass estimates (in kDa units).

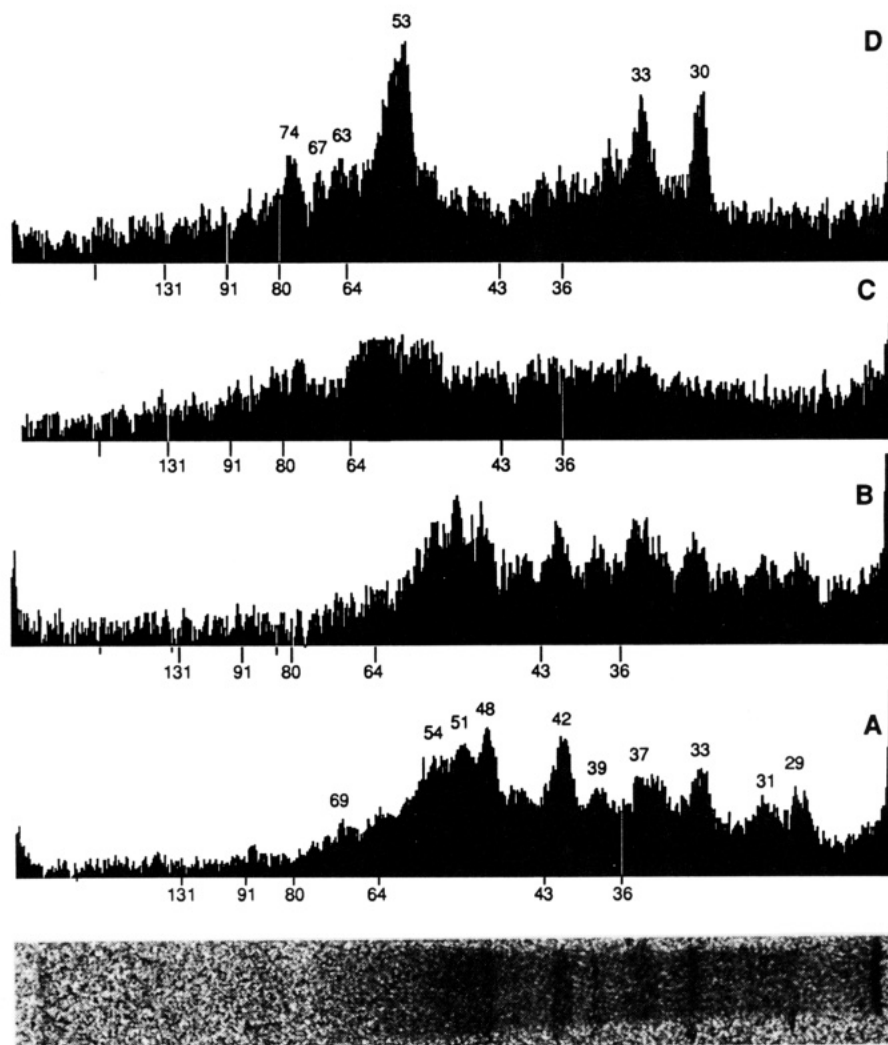


Figure 4. Protein adducts in mouse liver mitochondria. Radioactivity profiles obtained by storage phosphor analysis of proteins separated by denaturing SDS-PAGE and transferred to nitrocellulose. Samples contained $\sim 300 \mu\text{g}$ of protein from mice treated with the compounds in Table 1. (A) Ring-APAP; (B) acetyl-APAP; (C) AMAP; (D) low-dose APAP. Hash marks below the profiles indicate the positions of molecular mass standards, 180, 131, 91, 80, 64, 43, and 36 kDa, that were run in a parallel lane. Peaks are annotated with the corresponding molecular mass estimates (in kDa units).

proteins were transferred from the gel to nitrocellulose membranes for autoradiography. Although some protein is lost in the process of transfer, the accumulation of protein on the surface of the membrane increases the sensitivity to autoradiography that utilized a storage phosphor screen which was "read" by a laser. This technique differs from traditional autoradiography with X-ray film in that the response is linear throughout the dynamic range and is more sensitive (41). Radioactivity profiles could be obtained in this manner in less than 4 days. Similar results by traditional autoradiography/fluorography took up to 4 months. One disadvantage to the PhosphorImager is that exposures longer than 4 days did not increase the signal-to-background ratio.

Histograms of radioactivity as a function of migration distance are shown in Figure 3. The major APAP adduct was to a protein (proteins) in the 52–58 kDa range (Figure 3A). This band contains about 40% of the radioactivity as determined by integration of the trace. Acetyl-labeled APAP had an almost identical spectrum (Figure 3B).

The major adduct formed from AMAP apparently has the same M_r as that of APAP (Figure 3C). However, an adduct of ~ 27 kDa was more abundant in the APAP sample than in the AMAP sample, whereas an adduct of ~ 140 kDa was more abundant in the AMAP sample than

in the APAP sample. In general, however, the adducts found in the cytosolic fraction are similar for both APAP and AMAP although the intensity of AMAP adduct peaks is lower. This decreased signal-to-noise of AMAP samples relative to the APAP samples may be due to a decreased specificity in the formation of adducts, or it may be due to degradation of the adducts during sample workup and electrophoresis. The former possibility was addressed by 2-D electrophoresis, and the latter possibility was addressed by a determination of the amount of AMAP-protein adducts that could be recovered from SDS-PAGE gels (forthcoming Discussion).

The low dose of APAP apparently produced fewer adducts. Conspicuously absent from the trace (Figure 3D) are adducts at ~ 31 and ~ 99 kDa which are present after a toxic dose of APAP (Figure 3A). The signal-to-noise ratio, and therefore apparent resolution of peaks, are greater for protein adducts after this low dose of APAP compared to AMAP because the specific activity of the radiolabeled compound used was more than double that of the ring-labeled AMAP.

SDS-PAGE of Proteins from the Mitochondrial Fraction. The mitochondrial fraction is of interest because of the reports of mitochondrial damage during APAP toxicity (21, 42–46). AMAP, on the other hand, does not cause mitochondrial damage or hepatotoxicity

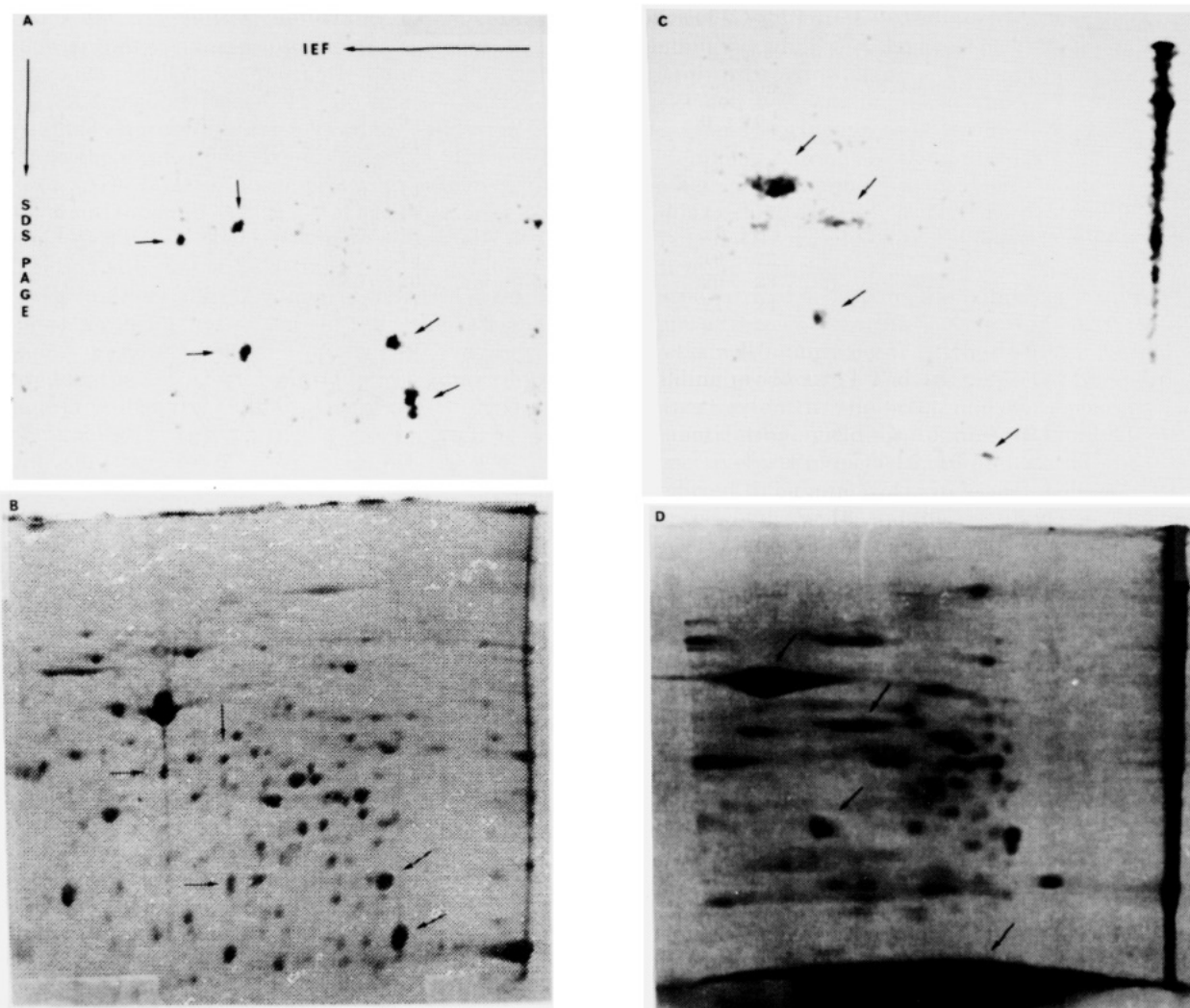


Figure 5. Comparison of APAP and AMAP adducts in mouse liver cytosol by 2-D gel electrophoresis. (A) Autoradiogram of APAP gel; (B) Coomassie Blue stain of APAP gel; (C) autoradiogram of AMAP gel; (D) Coomassie Blue stain of AMAP gel. Protein samples were focused (x -axis, cathode on the right) and then separated by SDS-PAGE (y -axis, dye front at the bottom). Arrows indicate correspondences between gels A and B and between gels C and D.

until glutathione is severely depleted in the mitochondria (47). Relative to the cytosol, less protein from this fraction could be loaded without a severe decrease in resolution. Thus, the amount of radioactivity is low, but peaks are discernible. Binding of radiolabel from both [*ring*- ^{14}C]APAP (Figure 4A) and [*acetyl*- ^{14}C]APAP (Figure 4B) was similar and is characterized by a triad of peaks at 54, 51, and 48 kDa, as well as peaks at 69, 42, 37, 33, 31, and 29 kDa. The intensity of AMAP binding (Figure 4C) was so low as to preclude any meaningful resolution of identifiable protein adducts, consistent with results of previous studies which showed that reactive metabolites of AMAP bound to mitochondrial proteins to a significantly lesser extent than reactive metabolites of APAP (21).

The low-dose APAP profile shows the greatest selectivity in binding to the mitochondrial fraction (Figure 4D). A large peak at 53 kDa is evident, as are peaks at 74, 67, 63, 33, and 30 kDa. These results are consistent with those of the cytosolic sample in which the low dose of APAP yields fewer adducts. Again, it should be noted that the specific activity of APAP used in the low-dose study was more than double that of the APAP used in the high-dose study.

Two-Dimensional Electrophoresis of Cytosolic Protein. Cytosolic fractions from APAP treated and AMAP treated animals were subjected to isoelectric

focusing followed by SDS-PAGE. In general, a large number of adducts could be observed in the 2-D image (Figure 5A) that contribute to the complexity of the SDS-PAGE (1-D) profiles (Figure 3A). A rough calibration of molecular size indicates that the ~52 kDa adduct apparent on the SDS-PAGE (1-D) profile is made up of more than one adduct. From the 2-D image in Figure 5A it is apparent that the "noise" in the 1-D samples is largely a result of the complexity of the sample. A comparison of the Coomassie Blue staining of the same gel (Figure 5B) attests to the selectivity of APAP binding.

A comparison of APAP and AMAP binding to cytosolic protein was facilitated by running these two samples under identical conditions. The resulting radiograms and protein staining images after AMAP treatment are shown in Figure 5C,D. As was demonstrated by SDS-PAGE, the pattern of adducts formed from AMAP is comparable to that formed from APAP; however, there are some spots corresponding to APAP adducts that are not observed in the AMAP sample.

Recovery of Radioactivity from APAP and AMAP SDS-PAGE Gels. Although similar amounts of radiolabeled homogenate and cytosolic proteins from livers of mice treated with APAP and AMAP were loaded onto gels, the radiolabel associated with electrophoretically resolved bands of proteins was always greater for APAP than AMAP. One possible explanation is that AMAP

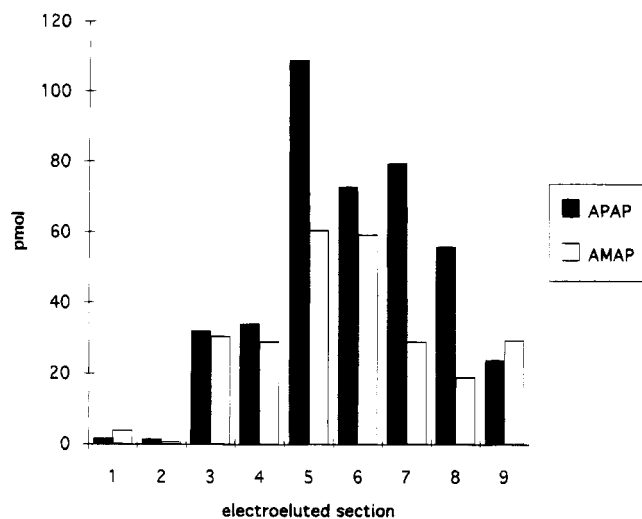


Figure 6. Recovery of radioactivity from SDS-PAGE gels of mouse liver cytosol. Protein was obtained from liver cytosols of mice 2 h after treatment with either APAP or AMAP. A sample of protein from each treatment (200 μ g representing ~600 pmol equivalents of APAP adduct and ~800 pmol equivalents of AMAP adduct) was subjected to denaturing SDS-PAGE. The tube gels were cut into 1 cm segments. The first two lanes of the x-axis correspond to the stacking gel, and lanes 3–9 are the separating gel. Radiolabeled protein was recovered by electroelution and counted by liquid scintillation counting. Total recovery of radiolabel was 66% for APAP and 32% for AMAP.

binding was less selective for individual protein targets such that the pattern of binding observed in SDS-PAGE gels was more diffuse. Alternatively, radioactivity may have been lost during sample preparation and/or electrophoresis owing to instability of the protein adducts.

To find out whether or not AMAP adducts were actually lost from protein during the process of electrophoretic analysis, we undertook a quantitative measurement of the radioactivity present in the SDS-PAGE gels of APAP and AMAP cytosolic protein. The application of a modest amount of protein (200 μ g/lane) ensured that all of the sample would enter the gel. Then, using electrophoretic extraction (electroelution) on gel slices, quantitative recovery of protein from the gel was facilitated. The size of the gel slices was relatively large due to the limiting sensitivity of liquid scintillation counting (LSC). The profiles of radioactivity are presented in Figure 6. They reflect the radioactivity obtained from gels that are otherwise blotted to give radioactivity traces (as in Figures 3–5). Given the decrease in resolution, the profiles obtained by electroelution/LSC compare favorably to those obtained by autoradiography.

Previous studies have demonstrated that covalent binding to the cytosol fraction is greater for AMAP than for APAP (21), and therefore, we expected the binding in Figure 6 to be generally higher for AMAP than for APAP. Apparently, AMAP protein adducts are degraded during the sample preparation or electrophoresis.

To examine this possibility, the total amount of adducts bound to the cytosol was determined by three different methods: (1) the traditional method of TCA precipitation and organic solvent extraction; (2) repeated washing of the protein with phosphate buffer and isolation by ultrafiltration; (3) recovery of adducts after SDS-PAGE. The specific content of APAP radiolabel bound to the protein fraction did not markedly change from one method of workup to another. In contrast, the specific content of AMAP radiolabel bound to the protein fraction was greatly reduced after ultrafiltration or when recovered from SDS-PAGE gels. The results are presented

Table 2. Covalent Binding of APAP and AMAP to Cytosolic Proteins Determined before and after Electrophoresis

method ^a	nmol of adduct/mg of protein	
	APAP	AMAP
TCA prepn	2.13	3.64
ultrafiltration	2.31	1.52
recovery from SDS-PAGE gels	2.04	1.30

^a See Experimental Procedures for a description of the methods used.

in Table 2. It appears that AMAP adducts were degraded either by proteolysis or by chemical degradation to compounds that passed through the Centricon-10 ultrafiltration membrane. The results also indicate that AMAP adducts are lost during either sample preparation or electrophoresis. Our experience with the diphenolic GSH conjugates of AMAP has shown that they are not as stable as the APAP-GSH conjugate.² Therefore, it appears that the decreased intensity on the gels observed for AMAP-protein adducts compared to APAP-protein adducts is primarily a result of greater lability of the AMAP-protein adducts under conditions of denaturation. In fact, the results of both the 1-D and 2-D electrophoresis indicate that APAP and AMAP have many common protein targets. Whether or not the apparent chemical instability of AMAP adducts has toxicological ramifications is not presently known.

Comparison of APAP-Protein Adducts Observed by Radiolabel Detection or Immunological Detection with Antibodies. In a broad sense, results of APAP-protein adduct detection by radiolabel detection and by immunological detection are similar inasmuch as specific protein targets are observed by both methods. Moreover, both methods detect dominant adducts between 50 and 60 kDa in the cytosol. However, the percentage of the total adducts represented by this peak is only 40% of the cytosolic fraction, based on radiometric detection, whereas Bartolone et al. (22) reported that this adduct comprised up to 85% of the total adducts. As stated previously, immunological methods may not detect all adducts.

In order to make a direct comparison between the two methods, blots of liver cytosolic proteins from APAP treated mice were subjected to both autoradiography and antibody staining using an antibody raised to an APAP-protein conjugate (22). In this direct comparison the antibody recognized all of the major APAP—but not AMAP—bound cytosolic protein adducts (Figure 7). Moreover, the two methods compared reasonably well quantitatively, though there were some differences observed (Figure 8). For example, the major adduct(s) at a molecular mass of \approx 50–55 kDa (Figure 7) or $R_f \approx$ 0.6–0.7 (Figure 8) accounted for approximately 40–50% of the total radiolabel by phosphorimage analysis, whereas it accounted for 60–65% by densitometric analysis of the Western blots.

Discussion

It is clear from 2-D electrophoretic studies of liver proteins from B6C3F1 mice administered unlabeled APAP and AMAP that APAP treatment caused significant increases and decreases in the intensities of more protein spots than AMAP and that the AMAP changes generally occurred in a subset of those proteins modified by APAP (Figures 1 and 2). The same conclusion can be

² Unpublished results.

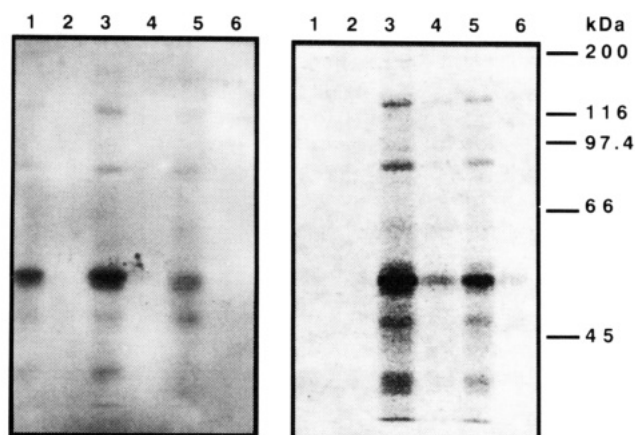


Figure 7. Comparison of immunodetection (left panel) and phosphorimage analysis (right panel) of APAP and AMAP adducts to proteins in mouse liver cytosol. The lanes in each panel are as follows: lane 1, 100 μ g of liver cytosolic protein from naive mice taken 2 h after the administration of 600 mg/kg of unlabeled APAP; lane 2, 100 μ g of liver cytosolic protein from naive mice taken 2 h after the administration of saline; lane 3, 100 μ g of liver cytosolic protein from phenobarbital treated mice taken 2 h after the administration of 250 mg/kg [14 C]APAP; lane 4, 100 μ g of liver cytosolic protein from phenobarbital treated mice taken 2 h after the administration of 600 mg/kg [14 C]AMAP; lanes 5 and 6 are the same as lanes 3 and 4, respectively, except that only 50 μ g of protein was applied to each lane. Immunodetection was accomplished by Western blotting as previously described (22). Phosphorimage analysis was carried out as described in Figure 3.

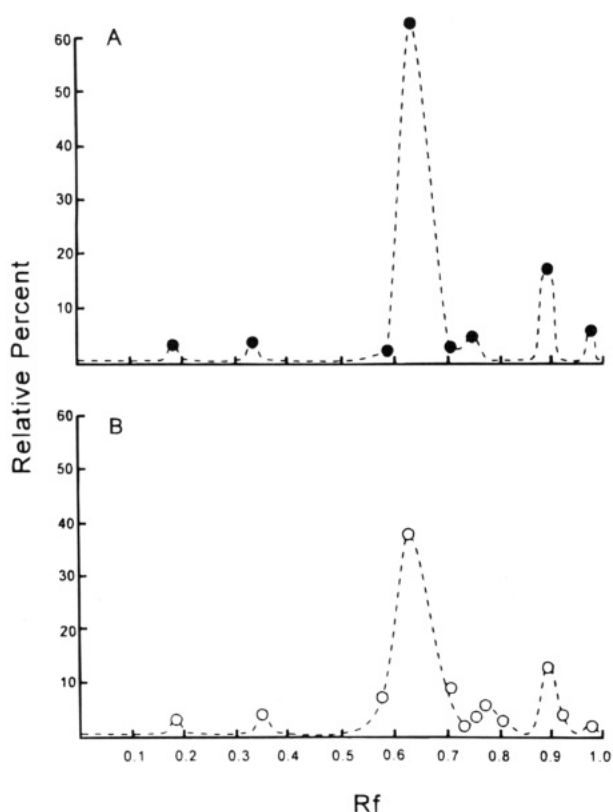


Figure 8. Relative percent of APAP protein adducts in mouse liver cytosol vs migration distance on SDS-PAGE gels based on (A) densitometric analysis of immunodetectable proteins in lane 3 of the left panel of Figure 7, and (B) phosphorimage analysis of radiolabeled proteins in lane 3 of the right panel of Figure 7.

drawn from phosphorimage analysis of radiolabeled protein adducts separated by 2-D gel electrophoresis from livers of mice treated with radiolabeled APAP and AMAP (Figure 5). However, the results of these latter studies cannot be compared directly on a one-to-one adduct basis

with the studies in the ISO-DALT system because the latter system requires samples from several individual animals and is optimized for computer quantitation of protein stain, whereas we could only use a couple of mice in the radiolabel studies because of limitations on amount of label available, and the 2-D system used was not optimized for computer quantitation but rather for heavy protein loading to obtain enough counts per adduct for reasonable detection. A series of 7 proteins in the molecular mass range 52–58 kDa showed changes in the 2-D gels used in the ISO-DALT system, the same range where 40% of the adducted APAP was bound. Due to the short time between treatment and collection of tissue (2 h), it is unlikely that these changes represent *de novo* protein synthesis, but rather that they represent shifts of material between locations on the 2-D gel due to adduction, cleavage, or other modification processes. In cases such as that of spot 952, which appeared only after APAP treatment, we searched for, but were unable to locate, a correspondingly diminished protein spot at a similar MW and nearby isoelectric point, as would be expected if spot 952 were an adducted version of another protein and a majority of that protein were altered by adduct binding. Unfortunately, spot 952 is close in MW and isoelectric point to a series of major proteins (including cytokeratins) that could obscure such a “parent” spot. An alternative possibility is that spots such as 952 are adducts of an abundant nearby spot, only a small part of which is altered. This alternative, if correct, would seem to argue that formation of such a spot is of minor biochemical importance, since a majority of the protein remains unaffected.

At this stage, only a limited number of proteins have been identified in the ISO-DALT 2-D maps: of those seen to change with APAP or AMAP, only serum albumin and cytochrome *b5* are known. The changes in albumin are likely to reflect alterations in the amount of blood in the organ and thus probably do not represent direct evidence of interesting biochemical effects, though they may point to important physiology. The remaining changes, however, appear to represent increases or decreases in authentic liver proteins that may or may not be caused by stable adduct formation and indicate that many more proteins are modified in some way by APAP treatment than can presently be accounted for by adduct formation as detected either radiochemically or immunochemically.

In the early 1970s, Mitchell et al. (2) put forth the hypothesis that a reactive, oxidative metabolite of APAP was generated in hepatocytes by cytochromes P-450 and bound to hepatocellular proteins, thereby initiating events that caused lethal injury to the hepatocytes. Several lines of evidence are consistent with this hypothesis. Among them are that both autoradiographical (17) and immunochemical (22, 28) detection methods have localized the protein-bound adducts to hepatocytes in the centrilobular region of the liver, wherein cells suffer acute lethal injury after APAP administration. Moreover, pretreatments of animals with agents that either increase or decrease APAP reactive metabolite formation increase and decrease in parallel the binding to proteins in hepatocytes and hepatocellular damage (17).

However, one criticism of the hypothesis that covalent protein binding of APAP metabolites is necessary for cell death has arisen because metabolites of the regioisomer, AMAP, bind extensively to hepatocytes without causing hepatocellular injury (21, 48). Therefore, the covalent binding of radiolabeled APAP and AMAP to hepatocellular proteins was examined by electrophoresis in order

to determine whether or not there were observable differences in covalent binding to protein targets.

Results of our studies clearly demonstrate that although several proteins appear to be common targets for APAP and AMAP reactive metabolites, there are both qualitative and quantitative differences in binding between the two regioisomers, and in addition, AMAP-derived protein adducts appear to be less stable than APAP-derived protein adducts. In cytosolic fractions of livers taken 2 h after treatment of mice with hepatotoxic doses of APAP and doses of the nonhepatotoxic AMAP that gave approximately the same total levels of protein adducts, major proteins of estimated molecular mass = 50–56 kDa were observed that accounted for approximately 25% of the total adducts in whole homogenate (data not shown) and 40% of the cytosolic protein adducts (Figure 3).

A major protein in this fraction that forms adducts with APAP reactive metabolites has been identified as a selenium binding protein (29, 30). The major cytosolic protein adducts formed with reactive metabolites of AMAP also are in the molecular mass = 50–56 kDa range (Figure 3C) and likely include the same selenium binding protein (49). If this is the case, either binding to this protein is not important in the pathogenesis of toxicity or factors other than binding are important. One possibility is that APAP reactive metabolites cause more damage by protein thiol oxidation as has been observed on a gross scale (50, 51). In fact, evidence has been presented that the major cytosolic protein arylated by APAP also is S-thiolated (52). Alternatively, this protein may simply serve as a detoxifying nucleophilic scavenger of reactive electrophilic metabolites of APAP, as suggested by extensive arylation of proteins of this approximate molecular weight after low, nontoxic doses of APAP in mice (Figure 3D). Another possibility recently set forth (49) is that more than one protein is present in this gel region and that the major protein is adducted by both APAP and AMAP, but that the other protein is not adducted significantly by AMAP. It also has been suggested that this protein may play a role in toxicity inasmuch as it translocates to the nucleus after adduction by APAP (33). Unfortunately, results of phosphorimage analysis of our 2-D gels did not clearly resolve these proteins, and as mentioned above, some AMAP adducts in this region of the gel were found to be less stable to the conditions of isolation and analysis.

Although there are a few marked differences in mouse liver cytosolic proteins arylated by APAP and AMAP (e.g., significantly more binding of APAP reactive metabolites to proteins of molecular mass \approx 27 and 195 kDa, Figure 3, and differences noted in 2-D chromatograms, Figure 5), the most pronounced quantitative differences were observed in the proteins of the mitochondrial fraction (Figure 4). This was anticipated since overall binding of AMAP reactive metabolites to mitochondrial proteins had previously been found to be 50–75% less than that of APAP reactive metabolites (21). APAP is known to cause lowered rates of mitochondrial respiration, decreased activities of mitochondrial electron transport enzymes, changes in mitochondrial electron transport enzymes, and changes in mitochondrial calcium homeostasis prior to cell death (21, 42–46). In contrast, AMAP does not cause mitochondrial damage and cell death unless mitochondrial glutathione is depleted (47). However, when reactive metabolites of AMAP are incubated directly with mouse liver mitochondria, they are as effective at inhibiting mitochondrial respiration as reac-

tive metabolites of APAP (53), and when incubated with mouse hepatocytes are as cytotoxic as well (54). Thus, identification of the specific proteins in the hepatic mitochondrial fraction that become arylated by APAP reactive metabolites is of interest. It should be noted that we also attempted to compare the binding of APAP and AMAP reactive metabolites to microsomal proteins. However, background levels of binding of both compounds to proteins in this fraction was high enough to obscure any meaningful interpretation of the data.

In summary, several radiolabeled protein adducts of APAP in mouse liver have been separated and characterized electrophoretically. Many of these adducts have been detected immunochemically by other investigators. The results of our studies that compared radiometric detection and immunodetection with one of these antibodies showed generally good agreement in detecting various adducts with some minor quantitative differences. Therefore, the immunochemical approach is very useful in characterizing adducts because it is more economical and easier to use. Also, it is not dependent upon the administration of radiolabeled APAP, which is an important consideration for human studies. In the final analysis, a combination of approaches will be needed to identify and characterize the many proteins that are apparently modified by APAP reactive metabolites, and to assess their role in APAP-mediated hepatotoxicity.

Acknowledgment. This research was supported by NIH Grant GM25418 (S.D.N.). We also acknowledge the excellent technical assistance of Ms. Cindy Chernoff and Ms. Mary Bruno.

References

- Boyd, E. M., and Berezky, G. M. (1966) Liver necrosis from paracetamol. *Br. J. Pharmacol.* **26**, 606–614.
- Mitchell, J. R., Jollow, D. J., Potter, W. Z., Davis, D. C., Gillette, J. R., and Brodie, B. B. (1973) Acetaminophen-induced hepatic necrosis. I. Role of drug metabolism. *J. Pharmacol. Exp. Ther.* **187**, 185–194.
- Hinson, J. A. (1980) Biochemical toxicology of acetaminophen. *Rev. Biochem. Toxicol.* **2**, 103–129.
- Prescott, L. F. (1983) Paracetamol overdose. Pharmacological considerations and clinical management. *Drugs* **25**, 290–314.
- Black, M. (1984) Acetaminophen hepatotoxicity. *Annu. Rev. Med.* **35**, 577–593.
- Miner, D. J., and Kissinger, P. T. (1979) Evidence for the involvement of *N*-acetyl-*p*-benzoquinone imine in acetaminophen metabolism. *Biochem. Pharmacol.* **28**, 3285–3290.
- Blair, I. A., Boobis, A. R., Davies, D. J., and Cresp, T. M. (1980) Paracetamol oxidation: Synthesis and reactivity of *N*-acetyl-*p*-benzoquinone imine. *Tetrahedron Lett.* **21**, 4947–4950.
- Corcoran, G. B., Mitchell, J. R., Vaishnav, Y. N., and Horning, E. C. (1980) Evidence that acetaminophen and *N*-hydroxyacetaminophen form a common arylating intermediate, *N*-acetyl-*p*-benzoquinone imine. *Mol. Pharmacol.* **18**, 536–542.
- Dahlin, D. C., and Nelson, S. D. (1982) Synthesis, decomposition kinetics, and preliminary toxicological studies on pure *N*-acetyl-*p*-benzoquinone imine, a proposed toxic metabolite of acetaminophen. *J. Med. Chem.* **25**, 885–886.
- Dahlin, D. C., Miwa, G. T., Lu, A. Y. H., and Nelson, S. D. (1984) *N*-Acetyl-*p*-benzoquinone imine: A cytochrome P-450-mediated oxidation product of acetaminophen. *Proc. Natl. Acad. Sci. U.S.A.* **81**, 1327–1331.
- Holme, J. A., Dahlin, D. C., Nelson, S. D., and Dybing, E. (1984) Cytotoxic effects of *N*-acetyl-*p*-benzoquinone imine, a common arylating intermediate of paracetamol and *N*-hydroxyacetaminophen. *Biochem. Pharmacol.* **33**, 401–406.
- Harvison, P. J., Guengerich, G. P., Rashed, M. S., and Nelson, S. D. (1988) Cytochrome P-450 isozyme selectivity in the oxidation of acetaminophen. *Chem. Res. Toxicol.* **1**, 47–52.
- Albano, E., Rundgren, M., Harvison, P. J., Nelson, S. D., and Moldéus, P. (1985) Mechanisms of *N*-acetyl-*p*-benzoquinone imine cytotoxicity. *Mol. Pharmacol.* **28**, 306–311.
- Boobis, A. R., Fawthrop, D. J., and Davies, D. S. (1989) Mechanisms of cell death. *Trends Pharmacol. Sci.* **10**, 275–280.

- (15) Nelson, S. D. (1990) Molecular mechanisms of the hepatotoxicity caused by acetaminophen. *Semin. Liver Dis.* **10**, 267–278.
- (16) Corcoran, G. B., and Ray, S. D. (1992) The role of the nucleus and other compartments in toxic cell death produced by alkylation hepatotoxicants. *Toxicol. Appl. Pharmacol.* **113**, 167–183.
- (17) Jollow, D. J., Mitchell, J. R., Potter, W. Z., Davis, D. C., Gillette, J. R., and Brodie, B. B. (1973) Acetaminophen-induced hepatic necrosis. II. Role of covalent binding *in vivo*. *J. Pharmacol. Exp. Ther.* **187**, 195–202.
- (18) Potter, W. Z., Thorgeirsson, S. S., Jollow, D. J., and Mitchell, J. R. (1974) Acetaminophen-induced hepatic necrosis, covalent-binding and glutathione depletion in hamsters. *Pharmacology* **12**, 129–143.
- (19) Hoffman, K.-J., Streeter, A. J., Axworthy, D. B., and Baillie, T. A. (1985) Identification of the major covalent adduct formed *in vitro* and *in vivo* between acetaminophen and mouse liver proteins. *Mol. Pharmacol.* **27**, 566–573.
- (20) Rashed, M. S., Myers, T. G., and Nelson, S. D. (1990) Hepatic protein arylation, glutathione depletion and metabolic profiles of acetaminophen and a non-hepatotoxic regioisomer, 3'-hydroxyacetanilide, in the mouse. *Drug Metab. Dispos.* **18**, 765–770.
- (21) Tirmenstein, M. A., and Nelson, S. D. (1989) Subcellular binding and effects on calcium homeostasis produced by acetaminophen and a non-hepatotoxic regioisomer, 3'-hydroxyacetanilide. *J. Biol. Chem.* **264**, 9814–9819.
- (22) Bartalone, J. B., Sparks, K., Cohen, S. D., and Khairallah, E. A. (1987) Immunohistochemical detection of acetaminophen-bound liver proteins. *Biochem. Pharmacol.* **36**, 1193–1196.
- (23) Roberts, D. W., Pumford, N. R., Potter, D. W., Benson, R. W., and Hinson, J. A. (1987) A sensitive immunochemical assay for acetaminophen-protein adducts. *J. Pharmacol. Exp. Ther.* **241**, 527–533.
- (24) Bartalone, J. B., Birge, R. B., Sparks, K., Cohen, S. D., and Khairallah, E. A. (1988) Immunohistochemical analysis of acetaminophen covalent binding to proteins: Partial characterization of the major acetaminophen-binding liver proteins. *Biochem. Pharmacol.* **37**, 4763–4774.
- (25) Pumford, N. R., Hinson, J. A., Potter, D. W., Rowland, K. L., Benson, R. W., and Roberts, D. W. (1989) Immunochemical quantitation of 3-(cystein-S-yl)acetaminophen adducts in serum and liver proteins of acetaminophen-treated mice. *J. Pharmacol. Exp. Ther.* **248**, 190–196.
- (26) Bartalone, J. B., Cohen, S. D., and Khairallah, E. A. (1989) Immunohistochemical localization of acetaminophen-bound liver proteins. *Fundam. Appl. Toxicol.* **13**, 859–862.
- (27) Birge, R. B., Bartalone, J. B., Emeigh-Hart, S., Nishanian, E., Tyson, C. A., Khairallah, E. A., and Cohen, S. D. (1990) Acetaminophen hepatotoxicity: Correspondence of selective protein arylation in human and mouse liver *in vitro*, in culture and *in vivo*. *Toxicol. Appl. Pharmacol.* **105**, 472–482.
- (28) Roberts, D. W., Bucci, T. J., Benson, R. W., Warbritton, A. R., McRae, T. A., Pumford, N. R., and Hinson, J. A. (1991) Immunohistochemical localization and quantification of the 3-(cystein-S-yl)acetaminophen protein adduct in acetaminophen hepatotoxicity. *Am. J. Pathol.* **138**, 359–371.
- (29) Pumford, N. R., Martin, B. M., and Hinson, J. A. (1992) A metabolite of acetaminophen covalently binds to the 56 kDa selenium binding protein. *Biochem. Biophys. Res. Commun.* **182**, 1348–1355.
- (30) Bartalone, J. B., Birge, R. B., Bulera, S. J., Bruno, M. K., Nishanian, E. V., Cohen, S. D., and Khairallah, E. A. (1992) Purification, antibody production, and partial amino acid sequence of the 58-kDa acetaminophen-binding liver proteins. *Toxicol. Appl. Pharmacol.* **113**, 19–29.
- (31) Khairallah, E. A., Bulera, S. J., and Cohen, S. D. (1993) Identification of the 44-kDa acetaminophen binding protein as a subunit of glutamine synthetase. *Toxicologist* (Abstr.) **13**, 114.
- (32) Pumford, N. R., Halmes, N. C., Martin, B. M., and Hinson, J. A. (1994) Covalent binding to *N*-10-formyl tetrahydrofolate dehydrogenase following a hepatotoxic dose of acetaminophen. *Toxicologist* (Abstr.) **14**, 426.
- (33) Hong, M., Cohen, S. D., and Khairallah, E. A. (1994) Translocation of the major cytosolic acetaminophen (APAP) protein adducts into the nucleus. *Toxicologist* (Abstr.) **14**, 427.
- (34) Laemmli, U. K. (1970) Cleavage of structural proteins during the assembly of the head of bacteriophage T₄. *Nature* **227**, 680–685.
- (35) Anderson, N. L., Nance, S. L., Pearson, T. W., and Anderson, N. G. (1982) Specific antiserum staining of two-dimensional electrophoretic patterns of human plasma proteins immobilized on nitrocellulose. *Electrophoresis* **3**, 135–142.
- (36) O'Farrell, P. H. (1975) High resolution two dimensional electrophoresis of proteins. *J. Biol. Chem.* **250**, 4007–4021.
- (37) Anderson, N. L., Copple, D. C., Bendele, R. A., Probst, G. S., and Richardson, F. C. (1992) Covalent protein modifications and gene expression changes in rodent liver following administration of methapyrilene: A study using two-dimensional electrophoresis. *Fundam. Appl. Toxicol.* **18**, 570–580.
- (38) Anderson, N. G., and Anderson, N. L. (1978) Analytical techniques for cell fractions. XXI. Two dimensional analysis of serum and tissue proteins: Multiple isoelectric focusing. *Anal. Biochem.* **85**, 331–340.
- (39) Anderson, N. L., and Anderson, N. G. (1978) Analytical techniques for cell fractions. XXII. Two dimensional analysis of serum and tissue proteins: Multiple gradient-slab electrophoresis. *Anal. Biochem.* **85**, 341–354.
- (40) Anderson, N. L. (1988) *Two-Dimensional Electrophoresis: Operation of the ISO-DALT System*, Large Scale Biology Press, Washington, DC.
- (41) Johnston, R. F., Pickett, S. C., and Barker, D. L. (1990) Autoradiography using storage phosphor technology. *Electrophoresis* **11**, 355–360.
- (42) Dixon, M. F., Dixon, B., Aparicio, S. R., and Loney, D. P. (1975) Experimental paracetamol-induced hepatic necrosis: A light- and electron-microscope, and histochemical study. *J. Pathol.* **116**, 17–29.
- (43) Walker, R. M., Racz, W. S., and McElligott, M. D. (1980) Acetaminophen-induced hepatotoxicity in mice. *Lab. Invest.* **42**, 181–189.
- (44) Meyers, L. L., Beierschmitt, W. P., Khairallah, E. A., and Cohen, S. D. (1988) Acetaminophen-induced inhibition of hepatic mitochondrial respiration in mice. *Toxicol. Appl. Pharmacol.* **93**, 378–387.
- (45) Katiyare, S. S., and Satav, J. G. (1989) Impaired mitochondrial oxidative energy metabolism following paracetamol-induced hepatotoxicity in the rat. *Br. J. Pharmacol.* **96**, 51–58.
- (46) Burcham, P. C., and Harman, A. W. (1991) Acetaminophen toxicity results in site-specific mitochondrial damage in isolated mouse hepatocytes. *J. Biol. Chem.* **266**, 5049–5054.
- (47) Tirmenstein, M. A., and Nelson, S. D. (1991) Hepatotoxicity after 3'-hydroxyacetanilide administration to buthionine sulfoximine pretreated mice. *Chem. Res. Toxicol.* **4**, 214–217.
- (48) Roberts, S. A., Price, V. F., and Jollow, D. J. (1990) Acetaminophen structure-toxicity studies: *in vivo* covalent binding of a nonhepatotoxic analog, 3-hydroxyacetanilide. *Toxicol. Appl. Pharmacol.* **105**, 195–208.
- (49) Vecchiarelli, M. M., Tveit, A., Manatou, J. E., Khairallah, E. A., and Cohen, S. D. (1994) Discrimination among acetaminophen (APAP) hepatic protein targets: Mouse strain and APAP analog comparisons. *Toxicologist* (Abstr.) **14**, 427.
- (50) Tirmenstein, M. A., and Nelson, S. D. (1990) Acetaminophen-induced oxidation of protein thiols: contribution of impaired thiol metabolizing enzymes to the breakdown of adenine nucleotides. *J. Biol. Chem.* **265**, 3059–3065.
- (51) Nelson, S. D., Tirmenstein, M. A., Rashed, M. S., and Myers, T. G. (1990) Acetaminophen and protein thiol modification. In *Biological Reactive Intermediates IV* (Witmer, C. M., Snyder, R. R., Jollow, D. J., Kalf, G. F., Kocsis, J. J., and Sipes, I. G., Eds.) pp 579–588, Plenum Press, New York.
- (52) Birge, R. B., Bartalone, J. B., Cohen, S. D., Khairallah, E. A., and Smolin, L. A. (1991) A comparison of proteins S-thiolated by glutathione to those arylated by acetaminophen. *Biochem. Pharmacol.* **42**, 5197–5207.
- (53) Ramsay, R. R., Rashed, M. S., and Nelson, S. D. (1989) *In vitro* effects of acetaminophen metabolites and analogs on the respiration of mouse liver mitochondria. *Arch. Biochem. Biophys.* **273**, 449–457.
- (54) Holme, J. A., Hongslo, J. K., Bjorge, C., and Nelson, S. D. (1991) Comparative cytotoxic effects of acetaminophen, a non-hepatotoxic regioisomer, acetyl-*m*-amino phenol, and their postulated reactive hydroquinone and quinone metabolites in monolayer cultures of mouse hepatocytes. *Biochem. Pharmacol.* **42**, 1137–1142.

TX940050F